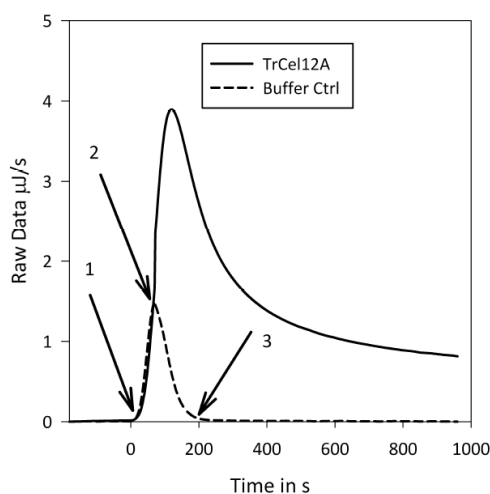


## Supplemental Data.

### Method Development.

#### Technical description of the method

See Fig S1. The data is presented as raw data as no calculation can be performed on the buffer injection to the RAC for comparative purposes. The 8 g/L RAC is added to the cell and allowed to come to thermal equilibrium at 30 °C. This is indicated by the flat baseline where the ITC is then set to monitor 180 s to provide a baseline for further calculations (-180 s to 0 s). Now the ITC stirring is turned on at 400 rpm and the enzyme is injected at  $t = 0$ , arrow [1]. This is followed by 60 s of intense mixing, and then the stirring is turned off as shown by arrow [2]. The thermal effects of the friction from stirring have disappeared after ca. 180 s, shown by arrow [3].



**Figure S1.** A typical ITC run as shown in Fig. 2 of the manuscript. RAC 8 g/L, pH 5.0 in 50 mM sodium acetate with 2 mM calcium chloride. Here the buffer control is an injection of the buffer with no enzyme to the 8 g/L RAC under the exact same conditions as enzymatic hydrolysis is performed. The same volume of buffer and enzyme are injected here, 10 µL to the 957 µL cell.

Fig. S1 illustrates some important principles of the assay. Firstly, the baseline after the injection of buffer returns to the same point after approximately 180 s, so the signal generated by the enzymatic reaction after this time is independent of stirring influences. Secondly, the peak of the enzyme injection is far higher than that of the buffer control. While there is an influence from the stirring, the heat generated in the first part of the ITC run exceeds any frictional interference. And finally, the interference from stirring is easily corrected for. All areas calculated from 0 to 230 s in the manuscript have been corrected for buffer to RAC injections areas, by subtracting the integral of the appropriate control injection.

## Calibration and Controls

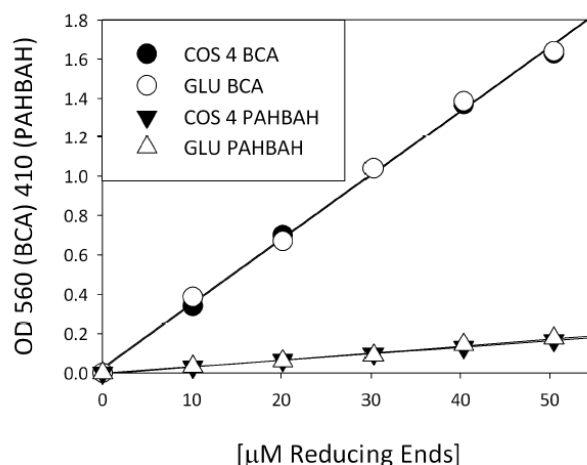


**Figure S2.** Calibration of the BCA and PAHBAH assays. GLU = glucose, COS 4 = Cellotetraose.

The PAHBAH and BCA assays were calibrated using both glucose (G1) and cellotetraose (G4) initially to determine the effect of soluble cello-oligosaccharide length on the spectrophotometric response. Both assays provided near identical calibration curves for the G1 and G4 standards; see Fig. S2. It was determined the PAHBAH assay was affected by the presence of mixtures of insoluble and soluble substrates, the two calibrations carried out in the absence and presence of RAC differing in slope values by a factor of 1.5. The BCA assay displayed no such bias, both glucose and cellotetraose calibrations in the presence and absence of RAC agreeing to within 8 %, and the recovery of 40  $\mu\text{M}$  cellotetraose with varied RAC background was complete,  $96 \pm 3\%$ . The BCA assay was approximately ten times more sensitive than the PAHBAH assay.

The sensitivity of the assays to mixtures of soluble and insoluble reducing ends was tested. To determine if the assays were affected by a constant RAC background, they were calibrated from 10  $\mu\text{M}$  to 50  $\mu\text{M}$  glucose and cellotetraose in the presence and absence of 1 g/L RAC. To test if the assays were incorrectly measuring mixtures of insoluble and soluble reducing ends 40  $\mu\text{M}$  of glucose or cellotetraose was added to varied amounts of RAC (0.2 – 1 g/L). The % recovery measured by determining how much of the added 40  $\mu\text{M}$  could be re-found in the mixtures after subtracting the background.

RAC effects

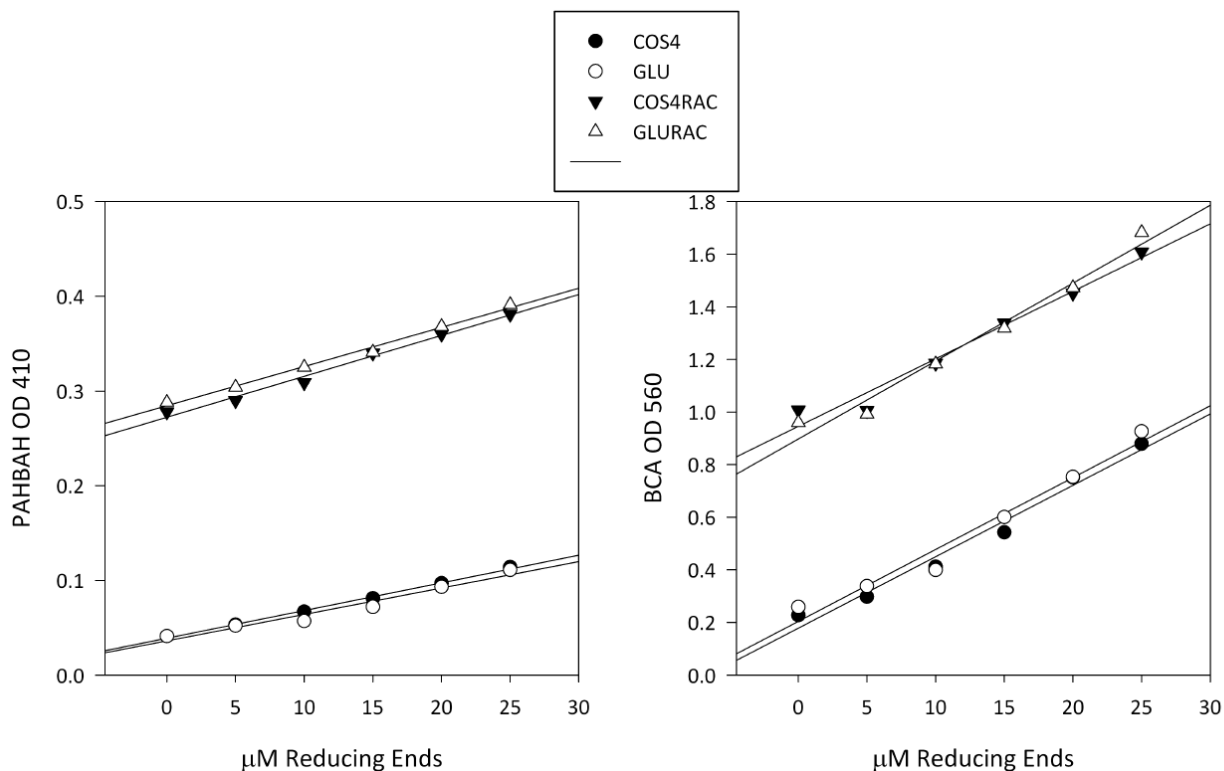


**Figure S3.** Both assays were calibrated with glucose and COS4 in the absence and presence of a 1.6 g/L RAC background, typical for assay conditions. The higher graph depicts the PAHBAH assay while the lower represents the BCA assay. GLU = glucose, COS4 = cellotetraose, GLURAC = glucose with added RAC, COS4RAC = Cellotetraose with added RAC.

As may be seen from the slopes, the PAHBAH (above, read at OD410) assay appears to overestimate the amount of reducing ends by a factor of 1.5 in the presence of RAC. All further assays were carried out with the BCA method.

Table S2 Slopes of calibrations in the presence of RAC.

PAHBAH		Error
COS4	2.92E-03	<b>1.48</b>
GLU	2.79E-03	<b>1.48</b>
COSRAC	4.32E-03	
GLURAC	4.13E-03	
BCA		Error
COS4	2.72E-02	<b>0.94</b>
GLU	2.73E-02	<b>1.08</b>
COSRAC	2.57E-02	
GLURAC	2.96E-02	

## Mixing and reaction quenching

The mixing effect was not a critical parameter in this set up. Samples analyzed directly from the ITC ( $\pm$  mixing, 400 rpm) produced the exact same amount of reducing ends to within 3 % (data not shown). In this assay set up it appears the initial mixing is sufficient to homogenize the enzymes and substrate, even at varying enzyme doses. In short, the heat signal directly reflects the hydrolysis of the amorphous substrate and may be converted to an enzymatic rate using the measured  $\Delta_{app}H$ .

It was found the 2 M  $\text{Na}_2\text{CO}_3$  was effective at quenching the reaction. No further activity was measured in samples allowed to stand at 30 °C for an extra 30 min compared to those measured immediately after quenching. Controls of enzyme added to "quenched" RAC were used to correct for protein background in the assay.

## Quantification of burst phase.

The extent of the burst phase, *i.e.* the number of glycosidic bonds hydrolyzed during the fast initial stage, was assessed in two ways.

First, inspection of Fig 2 empirically suggests that the width of the initial peaks is about 230 sec. Hence, we determined the area under the calorimetric signal from  $t=0$  to  $t=230$  s, and used this value,  $Q_{230}$ , to calculate the "concentration" of hydrolyzed glycosidic bonds,  $C_{hyd}^{230}$ , in the calorimetric cell after 230 s,

$$C_{hyd}^{230} = \frac{Q_{230}}{V_{cell} \Delta_{app} H}$$

Here  $\Delta_{app}H$  is the apparent enthalpy determined in Fig. 1 and  $V_{cell}$  is the volume of the calorimetric measuring cell (0.957 mL). It was found that  $C_{hyd}^{230}$  increased proportionally to the enzyme concentration and the coefficients were  $1239 \pm 200$  ( $n=18$ ) for *TrCel7B*,  $242 \pm 38$  ( $n=20$ ) for *TrCel5A* and  $280 \pm 29$  ( $n=5$ ) for *TrCel12A*, respectively.

To test the validity of the above calculation, we also used the established method to analyze the burst phase for soluble substrates (particularly in so-called active site titration; see *e.g.* pp 156-157 in ref. 1). Here, the idea is to plot the concentration of product as a function of time, and extrapolate the linear (steady-state) range to  $t=0$ . To do this, we first converted the ITC signals in Fig.2 to the temporal development in the "concentration" of hydrolyzed bonds,  $C_{hyd}(t)$ , again using the relationship,

$$C_{hyd}(t) = \frac{Q(t)}{V_{cell} \Delta_{app} H}$$

were plotted as a function of time and fits to the near-linear range (400-600 sec) was extrapolated to  $t=0$  as shown for *TrCel12A* in panel A of Fig. S4.

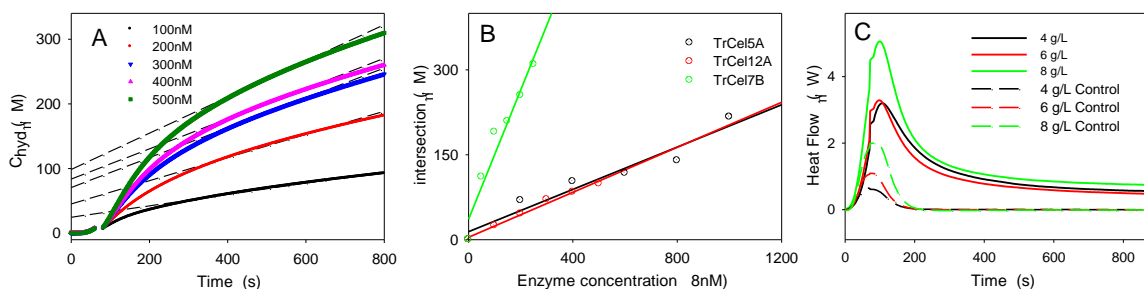


**Figure S4.** Dependence of the burst phase on the concentration of enzyme (panel A and B) and substrate (panel C). Panel A shows the “concentration” of hydrolyzed glycosidic bonds,  $C_{hyd}(t)$ , in the calorimetric experiments calculated from the data in Fig. 2, and plotted as a function of time. The enzyme was *TrCel12A* and the substrate was RAC, 8 g/L. The burst is defined as the intersection of the ordinate and the dashed line (specifying a near-steady state condition) and this intersection is plotted as a function of the enzyme concentration for all three enzymes in panel B. The slopes in this plot specify the number of glycosidic bonds hydrolyzed by one protein molecule during the burst. Panel C shows raw calorimetric data for hydrolysis experiments (*TrCel7B*) with three different substrate concentrations (full lines) and the corresponding control experiments (dashed lines). The hydrolytic activity is the difference between the full and the dashed curves.

The intersections defined in Fig. S4 A, scaled proportionally to the enzyme concentration for all three enzymes (Fig. S4 B). The slopes of the linear fits in panel B specify the numbers of hydrolytic cycles per enzyme during the burst, and the values were  $237\pm35$ ,  $223\pm20$  and  $1450\pm150$  for *TrCel5A*, *TrCel12A* and *TrCel7B* respectively. These values match the ones calculated by the first method.

The effect of varying substrate concentration is illustrated in panel C of Fig. S4. The full lines show results for the addition of 200nM *TrCel7B* to different RAC concentrations, and the dashed lines are the corresponding controls for the addition of buffer. It appears that the controls increase with the RAC concentrations due to the higher viscosity and concomitant increase in the heat produced during stirring (*c.f.* Fig S1). Integration of the difference between hydrolysis experiment and control over the first 230 sec showed a burst of 1310, 1150 and 1530 hydrolytic cycles per enzyme molecule for respectively 4, 6 and 8 g RAC/L. These numbers are in accord with the burst found in trials with variable enzyme concentration (described above), and we conclude that to within the experimental precision, the magnitude of the burst did not depend on the concentration of substrate in the investigated range.

#### Literature Values

**Table S1. Summary of some reported kinetic measurements for *TrEGs* action on cellulose.**

Enzyme	Temp.	Substrate/incubation time	Turnover	Ref.
<i>TrEG</i>	50 °C	Filter paper/1 h	$0.14 \text{ s}^{-1}$	(2)‡
<i>TrEG</i>	50 °C	Amorphous Cellulose/20 h	$2.8 \text{ s}^{-1}$	(3) ‡
<i>TrCel7B</i>	45 °C	Avicel/30 min	$0.13 \text{ s}^{-1}$	(4) ‡
		Amorphous Cellulose/30 min	$19.95 \text{ s}^{-1}$	
<i>TrCel7B</i>	40 °C	Avicel/8 h	$0.004 \text{ s}^{-1}$	(5) ‡
		Filter paper/8 h	$0.002 \text{ s}^{-1}$	
<i>TrCel7B</i>	50 °C	Avicel/120 h	$0.45 \text{ s}^{-1}$	(6) ‡
<i>TrCel7B</i>	50 °C	Filter Paper/40 min	$0.92 \text{ s}^{-1}$	(7) ‡
<i>TrCel5A</i>	50 °C	Filter Paper/40 min	$0.46 \text{ s}^{-1}$	
<i>TrCel7B</i>	25 °C	Amorphous Cellulose/5-10 s	$20 \text{ s}^{-1}$	(8)†
<i>TrCel5A</i>	25 °C	Amorphous Cellulose/5 – 10 s	$8 \text{ s}^{-1}$	

† These are values reported directly in the article.

‡ These are values calculated based on values reported in  $\mu\text{mol}/\text{mg}/\text{min}$  in (9) and for the purposes of calculation *TrCel7B* calculations were based on based on  $M_w = 46032 \text{ Da}$ , *TrCel5A*  $M_w = 42185 \text{ Da}$ .

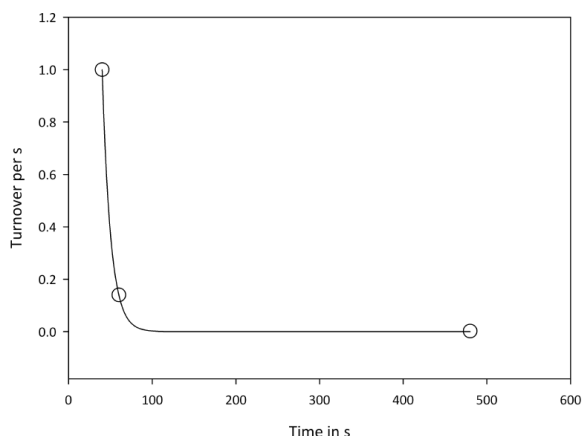


**Figure S5.** Based on reported values for filter paper. The reported values on this substrate vary from a turnover of almost  $1 \text{ s}^{-1}$  after 40 min to  $0.14 \text{ s}^{-1}$  after 1 h to  $0.002 \text{ s}^{-1}$  after 8 h. There will always be variation from assay type to assay type, and differences based on temperature, but these values constitute an exponential decay shown by the fitted line above. ( $R^2 = 0.93$ )

#### References for the Supplementary Data

1. Fersht, A. (1977) *Enzyme structure and mechanism*, second ed., W.H. Freeman and Company, New York
2. Ryu, D. D. Y., Kim, C., and Mandels, M. (1984) *Biotechnol. Bioeng.* **26**, 488-496
3. Nikupaavola, M. L., Lappalainen, A., Enari, T. M., and Nummi, M. (1985) *Biochem. J.* **231**, 75-81
4. Shoemaker, S., Watt, K., Tsitovsky, G., and Cox, R. (1983) *Bio-Technology* **1**, 687-690
5. Henrissat, B., Driguez, H., Viet, C., and Schulein, M. (1985) *Bio-Technology* **3**, 722-726
6. Baker, J. O., Ehrman, C. I., Adney, W. S., Thomas, S. R., and Himmel, M. E. (1998) *Appl. Biochem. Biotechnol.* **70-2**, 395-403
7. Nidetzky, B., Steiner, W., and Claeysens, M. (1994) *Biochem. J.* **303**, 817-823
8. Gruno, M., Valjamae, P., Pettersson, G., and Johansson, G. (2004) *Biotechnol. Bioeng.* **86**, 503-511
9. Zhang, Y. H. P., and Lynd, L. R. (2004) *Biotechnol. Bioeng.* **88**, 797-824